

Detergents Destabilize the Cubic Phase of Monoolein: Implications for Membrane Protein Crystallization

Y. Misquitta* and M. Caffrey*[†]

*Biophysics, [†]Biochemistry, and [‡]Chemistry, The Ohio State University, Columbus, Ohio 43210

ABSTRACT The in meso method for membrane protein crystallization uses a lipidic cubic phase as the hosting medium. The cubic phase provides a lipid bilayer into which the protein presumably reconstitutes and from which protein crystals nucleate and grow. The solutions used to spontaneously form the protein-enriched cubic phase often contain significant amounts of detergents that were employed initially to purify and to solubilize the membrane protein. By virtue of their surface activity, detergents have the potential to impact on the phase properties of the in meso system and, by extension, the outcome of the crystallization process. The purpose of this study was to quantify the effects that a popular series of nonionic detergents, the *n*-alkyl- β -D-glucopyranosides, have on the phase behavior of hydrated monoolein, the lipid upon which the in meso method is based. Phase identity and phase microstructure were characterized by small-angle x-ray diffraction on samples prepared to mimic in meso crystallization conditions. Measurements were made in the 0–40°C range. Samples prepared in the cooling direction allow for the expression of metastability, a feature of liquid crystalline phases that might be exploited in low-temperature crystallization. The results show that the cubic phase is relatively insensitive to small amounts of alkyl glucosides. However, at higher levels the detergents trigger a transition to the lamellar phase in a temperature- and salt concentration-dependent manner. These effects have important implications for in meso crystallization. A diffraction-based method for assaying detergents is presented.

INTRODUCTION

Lipidic mesophases have been employed in the production of membrane protein crystals for use in structure determination by crystallographic methods (Nollert et al., 2001; Rummel et al., 1998). The underlying mechanism of crystal growth, the role of the lipidic host, and indeed the exact nature of the mesophase from which the crystals grow are not known (Caffrey, 2000, 2002, 2003). Much effort is now being devoted to address these issues with a view to applying the method, hereafter referred to as the in meso method, to other membrane proteins in a more rational way.

As part of this endeavor, we are examining the role played by the various components likely to be included in the medium of a typical in meso crystallization trial. The nonionic detergents figure prominently here as a result of being used to isolate, purify, and solubilize membrane proteins. Thus, they are often carried along with the protein into the crystallization mix. Because of their surface activity, they are likely to have a profound effect on the mesophase characteristics of the crystallization medium and on the crystallization process itself. Indeed, it has been proposed that these adventitious materials play a role in in meso crystallization (Caffrey, 2000; Ai and Caffrey, 2000).

The medium-chain-length alkyl glycosides are the most commonly used nonionic detergents in membrane protein crystallization (Hunte and Michel, 2003). In a previous study, we examined the effect that one of these glycosides, DDM, had on the phase properties of hydrated MO, the lipid used for in meso crystallization. It was speculated that the lamellar phase stabilizing effect of the detergent might be integral to the crystallization process given that a lamellar-like portal may exist between the bulk cubic phase and the crystal surface (Ai and Caffrey, 2000; Caffrey, 2000).

The alkyl glucosides are a subset of the alkyl glycosides. They are related to DDM by having a polar head group consisting of a single glucose residue, where DDM has two. *n*-octyl- β -D-glucopyranoside, a representative alkyl glucoside, is the most extensively used of all detergents in membrane protein crystallization (Hunte and Michel, 2003). The alkyl chains in OG and DDM are 8 and 12 carbon atoms long, respectively. The effects that OG, and three of its commonly used alkyl chain homologs, have on the phase properties of hydrated MO were examined in the present study. To this end, small-angle x-ray diffraction was used for phase identification and microstructure characterization. Detailed phase diagrams of these three-component systems have been constructed. All four of the alkyl glucosides were tolerated to a limited degree in the hosting cubic phase of hydrated MO. However, as detergent concentration rose the cubic phase became unstable and eventually transitioned into the L_{α} phase in a temperature- and a salt concentration-dependent way. The implications these results have on membrane protein crystallization by the in meso method are discussed. Under certain conditions, the detergents were found to expand the unit cell size of the hosting cubic phase.

Submitted June 17, 2003, and accepted for publication July 24, 2003.

Address reprint requests to M. Caffrey, E-mail: caffrey.1@osu.edu.

Abbreviations used: DDM, *n*-dodecyl- β -D-maltopyranoside; DG, *n*-decyl- β -D-glucopyranoside; bR, bacteriorhodopsin; DOPC, dioleoyl phosphatidylcholine; DOPE, dioleoyl phosphatidylethanolamine; HG, *n*-hexyl- β -D-glucopyranoside; L_{α} , lamellar liquid crystal; Lc, lamellar crystal; LDAO, lauryldimethylamine oxide; MO, monoolein; NG, *n*-nonyl- β -D-glucopyranoside; OG, *n*-octyl- β -D-glucopyranoside; TLC, thin layer chromatography.

© 2003 by the Biophysical Society

0006-3495/03/11/3084/13 \$2.00

The possibility of using this effect as the basis for a detergent assay is examined.

In this study, phase behavior has been characterized in two ways. In the first, measurements were made in the heating direction starting at -15°C in the stable, low-temperature Lc phase. The second approach was used to represent metastable conditions. Here, data were collected in the cooling direction starting close to room temperature, the condition under which samples are prepared initially. The metastable mode allows for the expression of the natural undercooling tendency of the liquid crystal phases. As noted, this feature might be exploited in performing in meso crystallization at reduced temperatures (Caffrey, 2000).

MATERIALS AND METHODS

Materials

Monoolein (356.54 g/mol) was purchased at >99% purity (Nu Chek Prep, Elysian, MN, lots M-239-JAB-K and M-239-011-M) and was used without further purification. Purity was confirmed by TLC, as described (Misquitta and Caffrey, 2001). *n*-Decyl- β -D-glucopyranoside (320.4 g/mol, lot DG10), *n*-hexyl- β -D-glucopyranoside (264.4 g/mol, lot 6G02), lauryldimethylamine oxide (229.41 g/mol, lot LDA13), *n*-nonyl- β -D-glucopyranoside (306.4 g/mol, lot NG130), and *n*-octyl- β -D-glucopyranoside (292.4 g/mol, lot OG14) were purchased from Anatrace (Maumee, OH) at a reported purity of >99%, and were used without further purification. DOPC (786.12 g/mol, lot 181PC-138) and DOPE (744.03 g/mol, lot 181PE-102) were purchased from Avanti Polar Lipids (Alabaster, AL). Sodium dihydrogen phosphate dihydrate (156.01 g/mol, lot 424136/1, Fluka Chemie GmbH) and anhydrous dipotassium hydrogen phosphate (174.18 g/mol, lot 409672/1, Fluka Chemie) were obtained from Sigma-Aldrich (St. Louis, MO). Ammonium sulfate (132.14 g/mol, lot 124-1316) was purchased from Jenneile Chemical (Cincinnati, OH), and Bio-Beads SM-2 adsorbent was from Bio-Rad Laboratories (Hercules, CA). Water was obtained at a resistivity of >18 Mohm.cm from a Milli-Q water system (Millipore, Bedford, MA) consisting of a carbon filter cartridge, two ion exchange filter cartridges, and an organic removal cartridge.

Methods

Sample preparation

Samples for phase diagram construction were prepared at 60% (w/w) MO and 40% (w/w) alkyl glucoside solution, as described (Cheng et al., 1998; Ai and Caffrey, 2000). They were stored for no more than 12 h at room temperature ($\sim 21^{\circ}\text{C}$) before being used in low-angle x-ray diffraction measurements.

Samples in which the relative amounts of OG and MO were varied and where the total water content was held constant at 40% (w/w) were also prepared as part of this study. In this case, solid OG and MO were weighed into a Hamilton (Reno, NV) microsyringe (Cheng et al., 1998; Ai and Caffrey, 2000), and the requisite amount of water to produce a sample with 40% (w/w) water was added to a second microsyringe. The two syringes were coupled and the components were homogenized by mechanical mixing (Cheng et al., 1998).

Detergent assay

The detergent assay method uses samples prepared in an excess of a salt solution as follows. Dry MO (12 mg, 60% (w/w)) was combined with 8 mg (40% (w/w)) of a detergent solution prepared in 25 mM Na/K phosphate, pH 5.6, to create samples with detergent/MO ratios in the range from 0 to 0.32

mol/mol. Homogenization was done by mechanical mixing (Cheng et al., 1998). To this dispersion was added an excess (50 μL) of a concentrated salt solution, typically 2 M Na/K phosphate, pH 5.6. Again, homogenization was achieved by mechanical mixing as above. The sample (3–5 mg) was then transferred into and sealed in a 1-mm diameter x-ray capillary tube (Hampton Research, Laguna Niguel, CA) for diffraction measurements as described (Ai and Caffrey, 2000).

Additive effects on the detergent assay were evaluated in different ways, depending on additive type. Thus, for example, lipid additives such as DOPC and DOPE were combined with the MO in organic solvent before drying under vacuum and mixing with the detergent solution. Complete details of how such samples were prepared have been described (Cherezov et al., 2002). In contrast, protein and ammonium sulfate additives were combined with the detergent solution before mixing with MO in the concentrations required.

Bacteriorhodopsin

Purple membrane and purified bR (solubilized in OG) were prepared from *Halobacterium salinarum* strain S9 following published procedures (Dencher and Heyn, 1982). bR purity was evaluated by determining the ratio of the absorbance at 280 nm to that at 550 nm. A ratio of 1.5 was typically observed which corresponds to good quality protein (Dencher and Heyn, 1982). Absorbance at 550 nm was used to calculate moles of protein where the extinction coefficient is $58,000 \text{ M}^{-1} \text{ cm}^{-1}$ (Dencher and Heyn, 1982). The molecular weight of bR is $\sim 26 \text{ kDa}$ (Dencher and Heyn, 1982). The bR used in this study was dispersed in 25 mM Na/K phosphate, pH 5.6, at 10–26 mg protein/mL. The residual detergent concentration in the bR solution is described under Results.

Solubilized bR was stripped of excess detergent in a batch process by equilibrating the protein with Bio-Beads SM-2 adsorbent following supplier's instructions (Bio-Rad Labs, Hercules, CA). BioBeads were initially washed by vortex mixing with an excess of methanol (lot 023884, Fisher Scientific, Fair Lawn, NJ), and were then rinsed with water and slurried to remove excess water. The residual water content of the slurried beads was estimated by drying to be 10 mg water/g bead. The cleansed, moist beads were added to 300 μL bR solution (2 mg beads per 10 μL bR solution) and allowed to equilibrate at room temperature with continuous agitation. After 30 min, the beads were pelleted by spinning in a micro-centrifuge (Eppendorf Mini Spin Plus, Brinkmann, Westbury, NY) at 14,000 rpm for 2 min. The supernatant was removed and an $\sim 9\text{-}\mu\text{L}$ aliquot was taken for use in the detergent assay. Fresh, washed beads were added to the remaining supernatant (at a rate of 2 mg beads/10 μL bR solution) and detergent extraction continued with agitation for 30 min at which point the beads were pelleted by centrifugation as above. This extraction procedure and bead replenishment continued for up to 5 h. A control experiment was carried using a 0.46 M OG solution in 25 mM Na/K phosphate, pH 5.6, in place of the bR solution.

Membrane protein crystallization

bR crystallization was carried out at room temperature in a sample containing MO (60% (w/w)) and bR solution (40% (w/w)) at 25.6 mg protein/mL and 2.0–3.0 M Na/K phosphate, pH 5.6. The buffer was prepared by combining appropriate volumes of equimolar Na/H₂ phosphate and K₂/H phosphate solutions to achieve pH 5.6 and was filtered using a 22- μm syringe tip filter (Fisher Scientific, Fair Lawn, NJ). The MO and protein solution were homogenized by mechanical mixing (Cheng et al., 1998) at room temperature. The viscous mixture ($\sim 8 \text{ mg}$) was transferred to x-ray capillaries, as described above for diffraction measurements. A Na/K phosphate precipitant solution (pH 5.6) was placed in direct contact with the lipid/protein dispersion, and the capillaries were flame- and epoxy-sealed (Hampton Research). Crystals formed typically within two days and were visible upon inspection with a light microscope (Nikon Eclipse E400, NikonUSA, Melville, NY) at 100 \times magnification. Because the crystals are colored, they were clearly visible in the capillary despite being small.

Inspection of the sample between crossed polarizers was used to look for birefringent mesophases. Having the samples housed in capillaries meant that they could be used in x-ray diffraction measurements to follow mesophase behavior during protein crystallization.

Occasionally, crystallization was performed not in capillaries as above, but using home-made wells on glass microscope slides (Cherezov and Caffrey, 2003). In this case, the lipid/protein dispersion and precipitant volumes used were typically 70 nL and 1 μ L, respectively.

X-ray diffraction

Diffraction measurements as well as phase identification and microstructure characterization have been described (Caffrey, 1987; Ai and Caffrey, 2000). For the diffraction measurements, the minimum incubation period at each temperature was 3 h and exposure times were typically 30 min. The bulk of the phase diagram work was done by collecting data in the cooling direction to mimic conditions likely to prevail in handling samples for in meso crystallization (Qiu and Caffrey, 2000; Ai and Caffrey, 2000). As described below, this approach favors mesophase undercooling and metastability. In the interests of completeness, however, a limited number of measurements were made also in the heating direction. For this purpose, the OG/MO samples were cooled and incubated at -15°C for 4 h to induce solidification. Subsequent measurements were made in the heating direction from the low-temperature, Lc phase.

The reference state for this study is hydrated MO at 40% (w/w) water. At 20°C , such a system exists in the cubic-Pn3m phase. It is important to note that the phase behavior of the system is quite complex under these conditions and that slight changes in composition and/or temperature induces well defined changes in phase state and lattice parameter (Qiu and Caffrey, 2000). We have also found that the lattice parameter is sensitive to the lot number of the lipid. Indeed, in this study we have found that the phase microstructure of such a reference sample varied from 101 \AA to 106 \AA at 20°C . The error associated with the cubic-Pn3m phase lattice parameter value is $\pm 2.5 \text{\AA}$. The origin of such variation is not known. As noted above, we have tested the MO as supplied by the manufacturer and it is $>99\%$ pure, as judged by TLC.

RESULTS

Phase behavior studies

In what follows, we describe the phase behavior of the MO/water system as a function of temperature and detergent concentration. Samples were prepared at 60% (w/w) MO to model standard in meso crystallization conditions. We begin by presenting the results obtained with OG, the detergent most commonly used in membrane protein crystallization and the system investigated most extensively in this study.

Octyl glucoside/monoolein phase behavior in the heating direction

Fig. 1 A shows the partial phase diagram for the three-component system consisting of MO, OG, and water. The phase diagram was constructed in the heating direction from -15°C to 40°C in 5°C intervals. Incubation at -15°C for a minimum of 4 h induced the formation of the solid Lc phase which is the predominant phase at temperatures of 10°C and below (Fig. 1 A). The Lc phase has a lamellar repeat of $\sim 49.5 \text{\AA}$ that is insensitive to OG concentration and temperature. It converts to one or other of the liquid crystalline phases above 10°C . In the sample without OG, the

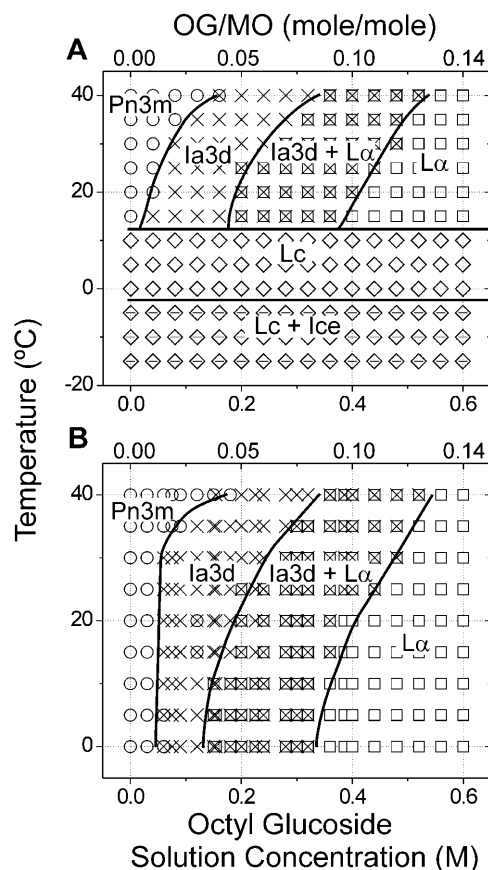


FIGURE 1 The identity and location in temperature-composition space of the various phases present in the MO/OG/water system determined by x-ray diffraction. Samples were prepared with 60% (w/w) MO and a 40% (w/w) aqueous solution of OG. (A) Measurements made in the heating direction from -15°C to 40°C . The identity of each of the phases is as follows: (\diamond) Lc, (\square) L_{α} , (—) ice, (\times) cubic-Ia3d, and (\circ) cubic-Pn3m. (B) Measurements made in the cooling direction from 30°C to -15°C , and in the heating direction from 25°C to 40°C . The identity of each of the phases is as follows: (\square) L_{α} , (\times) cubic-Ia3d, and (\circ) cubic-Pn3m. The samples were incubated at each temperature for a minimum of 4 h and exposed in the x-ray beam for diffraction measurement for a minimum of 30 min. The solid lines represent phase boundaries and are drawn to guide the eye.

pure cubic-Pn3m phase is stable in the $15\text{--}40^{\circ}\text{C}$ range as expected from the temperature-composition phase diagram for the two-component MO/water system (Briggs et al., 1996; Qiu and Caffrey, 2000). Adding OG triggers a series of phase transformations from the cubic-Pn3m (space group designation, Q^{224}) to the cubic-Ia3d (Q^{230}) phase, and finally to the L_{α} phase above an OG concentration of 0.40 M at 20°C . The detergent concentrations at which the different transitions occurred rose steadily with increasing temperature. At 40°C , the pure L_{α} phase emerged at $\sim 0.55 \text{ M}$ OG.

Octyl glucoside/monoolein phase behavior in the cooling direction

The partial metastable phase diagram of the MO/OG/water system was constructed using samples prepared initially at

room temperature (Fig. 1 *B*). The first measurements in this series were made at 30°C after a 4-h incubation of these freshly prepared samples. Subsequently, measurements were made in the cooling direction down to 0°C at intervals of 5°C with a minimum incubation period of 3 h at each temperature. To complete the phase diagram and to facilitate comparison with the data in Fig. 1 *A*, additional measurements were made on similar samples in the heating direction from 25°C to 40°C. The difference between this data set collected above 20°C and the corresponding set shown in Fig. 1 *A* is thermal history. The samples used to generate the $\geq 20^\circ\text{C}$ data in Fig. 1 *B* were never cooled below room temperature. Those in Fig. 1 *A* had been cooled initially to -15°C .

No significant differences in phase behavior were observed between the heating (Fig. 1 *A*) and the so-called metastable phase diagram (Fig. 1 *B*) in the temperature range above $\sim 20^\circ\text{C}$. However, substantial undercooling of all liquid crystal phases present was observed in the region below 20°C. Thus, in this mode of data collection, all three mesophases, the cubic-Pn3m, the cubic-Ia3d, and the L_α phases, persisted from 40°C down to 0°C. The L_c phase was not accessed under these metastable data collection conditions. The general trend observed under heating conditions for phase transitions to shift to lower OG concentrations with a reduction in temperature was also seen in the undercooled region from 20°C to 0°C. At 0°C, the lowest temperature examined in this mode, the pure L_α phase region was found to extend down to 0.35 M OG. The corresponding value at 40°C was 0.55 M OG.

Hexyl, nonyl, and decyl glucoside/monoolein phase behavior

The partial phase diagrams for these alkyl glucosides in combination with MO/water were constructed in the cooling direction to mimic conditions of use. The corresponding data in the temperature range from 0 to 35°C and in the composition range out to 0.6 M detergent are shown in Fig. 2. To facilitate comparisons, the cooling phase diagram for the OG-containing system is included in this figure. A perusal of the data shows that the behavior of the four alkyl glucosides is remarkably similar. Thus, in all cases increasing alkyl glucoside concentration triggers a sequential transformation from the cubic-Pn3m to the cubic-Ia3d to the L_α phase. Along the 20°C isotherm in Fig. 2, the Pn3m/Ia3d, Ia3d/(Ia3d + L_α), and (Ia3d + L_α)/ L_α transitions occur at ~ 0.05 M, 0.25 M, and 0.5 M alkyl glucoside, respectively, regardless of alkyl chain identity. Further, the transitions generally shift to higher detergent concentration with increasing temperature.

Mesophase microstructure

By way of characterizing phase microstructure, the lattice parameter of the different phases formed by the MO/alkyl

glucoside/water systems, and how they respond to temperature and composition, are presented here. Since most extensive data have been collected on the OG system, these are described first. Data are presented graphically and are also available in tabular form as Supplementary Material. In the interests of space, the corresponding data for the other alkyl glucoside systems are only available as Supplementary Material.

The lattice parameter data for the MO/OG/water system collected under conditions that include metastable behavior are presented graphically as a function of OG concentration and temperature in Fig. 3, *A* and *B*, respectively. It is interesting to note that whereas the detergent can induce phase transformations (Fig. 1), the microstructure of the individual phases does not change dramatically with OG concentration (Fig. 3 *A*). However, there is a general trend for the cubic phase lattice parameter to rise as OG level increases. At a given OG concentration, the effect of temperature is to reduce the lattice parameter of the cubic phases. The L_α phase shows little if any dependence on temperature in the range from 0°C to 40°C.

Since the samples used in preparing the heating and cooling phase diagrams were prepared at 40% (w/w) OG solution, the actual water content of samples containing OG is less than 40% (w/w). Further, the water content of the sample drops as the OG concentration in the solution rises. Therefore, the argument could be made that the effects seen on the phase behavior of the hydrated MO/OG system could be attributed not to OG but to an increase in lipid concentration relative to that of water as detergent concentration rises. To explore this possibility, samples were made in which the total water content was fixed at 40% (w/w) although the relative amounts of MO and OG were varied. The results (Fig. 4) show that the general phase behavior was no different from that observed when samples were prepared with a fixed amount of OG solution. Thus, OG triggers the familiar phase transition sequence: cubic-Pn3m to cubic-Ia3d to L_α . However, in the case where the water content of the sample was fixed at 40% (w/w), the lamellar phase showed a slight rise in repeat size with increasing OG levels that was not seen in samples prepared with 40% (w/w) OG solution.

The data for OG presented above are representative of those obtained with the other alkyl glucosides examined in this study.

Phase behavior in excess aqueous medium/detergent assay

In an earlier study, we observed that the lattice parameter of the cubic phase rose dramatically with DDM concentration (Fig. 4 *B* in Ai and Caffrey, 2000). The effect was seen when samples were prepared with an excess of aqueous medium. In contrast, the lattice parameter was relatively insensitive to detergent concentration under water-stressed conditions. In

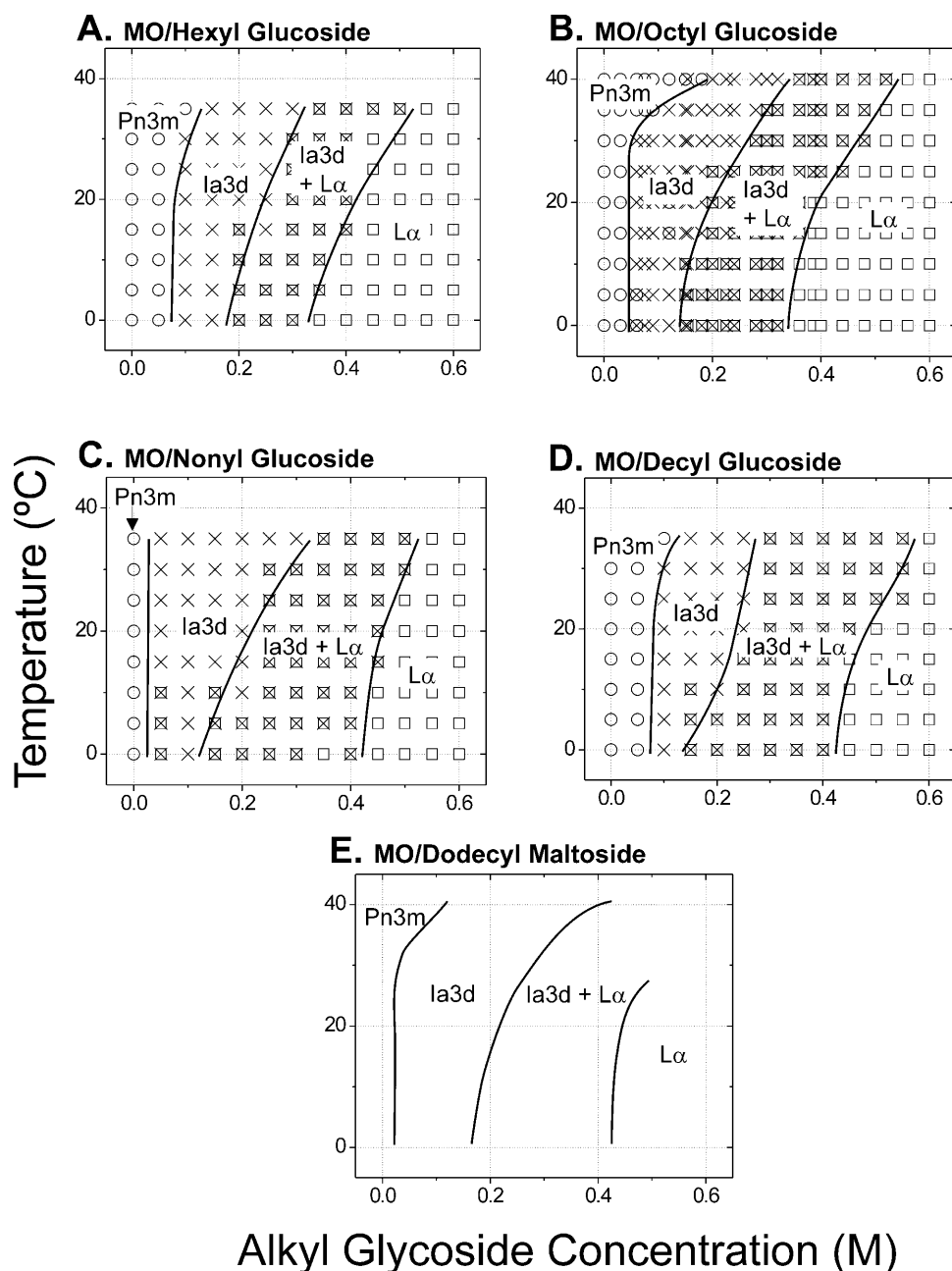


FIGURE 2 Cooling phase diagrams for the four alkyl glucosides and dodecylmaltoside. Temperature-composition phase diagrams for (A) the MO/HG/water system, (B) the MO/OG/water system, (C) the MO/NG/water system, and (D) the MO/DG/water system. (E) Interpreted phase diagram for the MO/DDM/water system. The identity of each of the phases is as follows: (\square) L_{α} , (\times) cubic- la_{3d} , and (\circ) cubic-Pn3m. The data in B are taken from Fig. 1 B. The data in E were redrawn from Ai and Caffrey (2000).

the current study, we investigated this effect further, focusing initially on the MO/OG system. The results show that the lattice parameter of the cubic-Pn3m phase in hydrated MO rises linearly with OG concentration under conditions of excess water (Fig. 5 A). That the system is fully hydrated is evidenced by the fact that bulk aqueous medium can be seen to coexist with the cubic mesophase after homogenization. The range of the linear response can be extended when the samples are prepared at high salt (2 M Na/K phosphate, pH 5.6) (Fig. 5 B). Beyond 1.18 M OG (0.28 mol OG/mol MO), the detergent triggers a transformation from the cubic-Pn3m to the L_{α} phase. A similar transition happens in the absence of salt but at a lower OG concentration (Fig. 5 A).

The sensitivity of the cubic phase lattice parameter to detergent suggested the possibility of using it as the basis for a detergent assay. Indeed, we have used it as a means for quantifying OG in different preparations of bR, and in bR fractions through the solubilization and purification procedures (unpublished work). We have long felt that residual OG in a preparation is a critical factor in determining bR crystallizability. This convenient assay enables us to evaluate the conjecture in a quantitative way.

In the current study, we used the detergent assay to determine the OG content of solubilized bR and to track its detergent load upon treatment with Bio-Beads SM-2. The data in Table 1 show that the original bR solution was 0.46

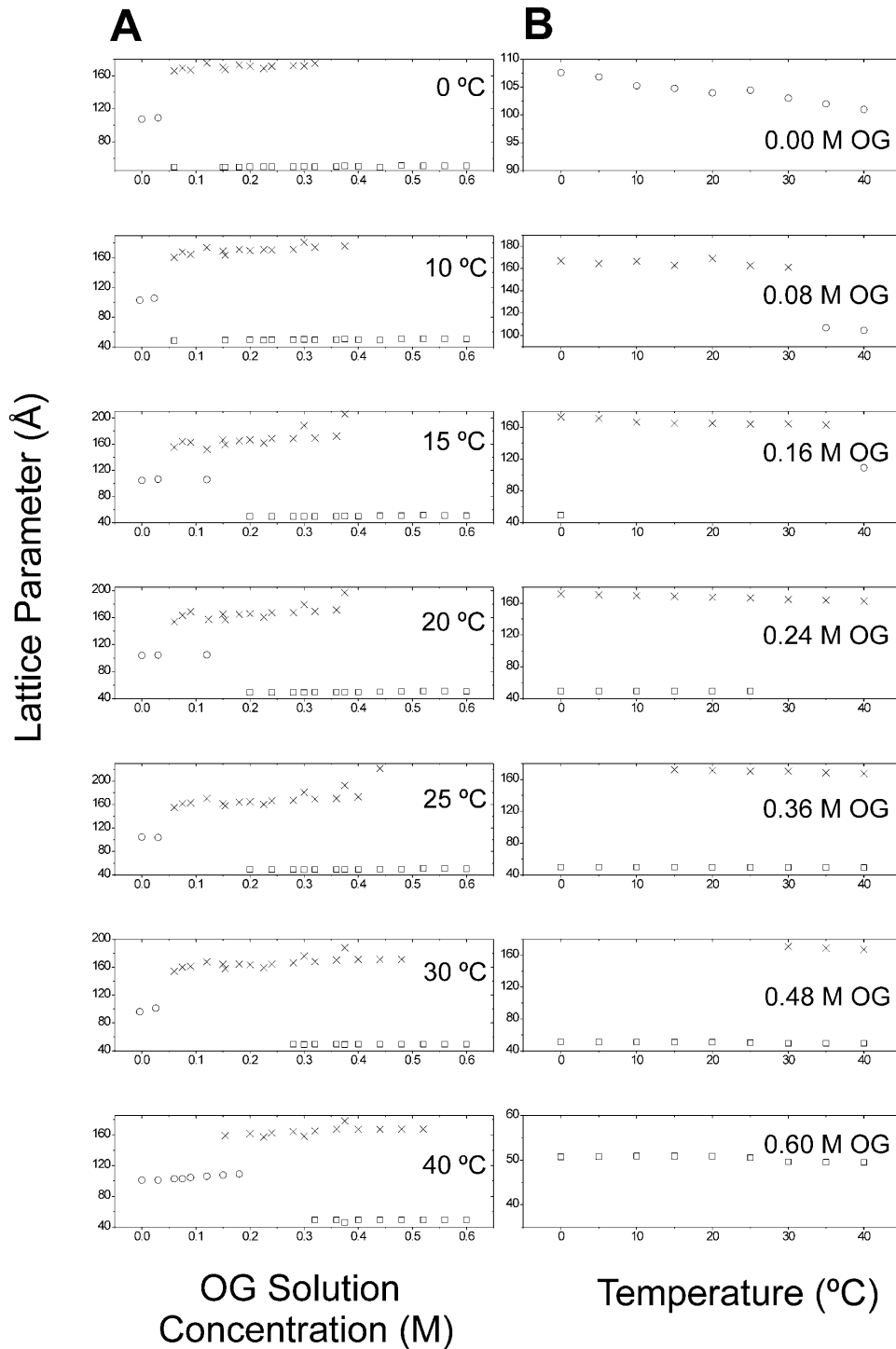


FIGURE 3 Detergent concentration dependence (A) and temperature dependence (B) of the lattice parameters of the phases found in the MO/OG/water system under heating (above 25°C) and cooling (metastable, 25°C and below) conditions at the indicated OG concentrations and temperatures. The identity of each of the phases is as follows: (□) L_{α} , (×) cubic-Ia3d, and (○) cubic-Pn3m. The structure parameter values reported are accurate to ± 1.0 Å for the L_{α} phase, and ± 2.5 Å for the cubic-Ia3d and cubic-Pn3m phases. The data in this figure correspond to those in Fig. 1 B.

M in OG. This corresponds to a detergent/protein mole ratio of 435:1. Upon treatment with Bio-Beads for several hours, the detergent was effectively stripped from the protein. In fact, the protein came out of solution after 3 h of treatment.

The effect seen with OG on the lattice parameter of the cubic phase of hydrated MO has been observed with the other alkyl glucosides examined in this study (data not shown) and is quite general. Indeed, the same effect is also

observed with a very different type of detergent, LDAO (Fig. 5 C).

With a view to evaluating the general applicability of the detergent assay, we have examined its sensitivity to a range of materials likely to accompany the detergent in biochemically relevant samples. Accordingly, the measurements were performed using samples containing OG and MO in the mole ratio range from 0.05 to 0.2 corresponding to the linear range

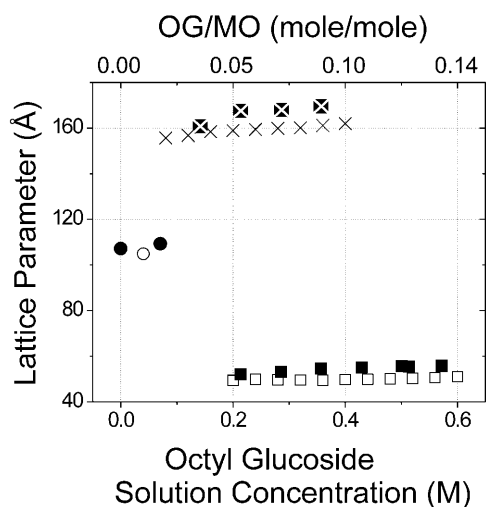


FIGURE 4 Dependence of mesophase lattice parameter on OG solution concentration at 20°C recorded under conditions where the water content (filled symbols) and the OG solution content (open symbols) of the sample were fixed at 40% (w/w). The identity of each of the phases is as follows: (□) L_{α} , (×) cubic-Ia3d, and (○) cubic-Pn3m.

of the standard curve in Fig. 5 *B*. The results show that low levels of the salt ammonium sulfate (Table 2), the lipids DOPC and DOPE (Table 3), and the water soluble protein lysozyme (Table 4) had little if any effect on assay sensitivity.

Mesophase transformations during in meso crystallization

As noted, the bR that is most commonly used in in meso crystallization studies is solubilized in OG. Thus, as protein concentration in the crystallization mix is elevated with a view to supersaturation, so too is the OG load on the system. The data in Fig. 1 show clearly that OG can destabilize the cubic phase, which presumably is integral to in meso crystallization. The possibility exists therefore that too high a protein concentration may raise the OG level concomitantly to the point where crystallization is hindered because of cubic phase destabilization. However, it has been proposed that a lamellar conduit exists between the crystal surface and the bulk cubic phase through which protein passes in the crystallization process (Caffrey, 2000). And thus, a lamellar phase may actually facilitate crystallization.

When in meso crystallization samples are prepared with low bR levels, the cubic phase is seen as expected. When viewed between crossed polarizers by polarized light microscopy such samples appear dark and featureless. The corresponding diffraction pattern verifies that the sample is cubic; in this case of the Pn3m type. In distinct contrast, at high bR concentrations, the samples develop the telltale L_{α} birefringence (Fig. 6 *A*). This is corroborated by diffraction

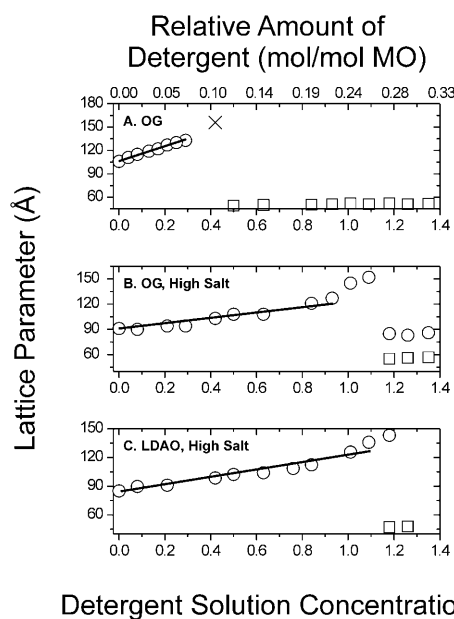


FIGURE 5 The phase microstructure detergent assay. Dependence of hydrated monoolein phase behavior on detergent concentration at 20°C in the presence of excess water (*A*) and an excess of 2 M Na/K phosphate, pH 5.6 (*B* and *C*). The detergents used were octyl glucoside (*A* and *B*) and LDAO (*C*). The identity of each of the phases is as follows: (□) L_{α} , (×) cubic-Ia3d, and (○) cubic-Pn3m. The solid lines superimposed on the cubic-Pn3m phase data represent a linear fit of form: $d_{100} = 96.4 M + 106$ in *A*, $d_{100} = 33.4 M + 91$ in *B*, and $d_{100} = 37.8 M + 85.1$ in *C*, where d_{100} is the lattice parameter of the cubic-Pn3m phase (in Å) and M is the molar concentration of the OG solution. The linear fit in *B* was from 0 to 0.93 M OG solution. The last two data points at 1.01 and 1.09 M OG solution were not included because the corresponding diffraction patterns consisted of a few relatively broad low-angle reflections and therefore their lattice parameters could not be accurately determined.

data showing either pure L_{α} phase or a coexistence of the L_{α} and cubic phases (Fig. 6 *B*). This result supports the view that OG accompanies bR into the in meso mix, and at high enough concentration partially or completely destabilizes the cubic in favor of the lamellar phase.

In meso crystal nucleation and growth in a system containing reconstituted bR is induced by the addition of a precipitant. Na/K phosphate, pH 5.6, in the concentration range from 2 to 3 M, serves the purpose. This is interesting in light of our findings that high salt concentration extends considerably the range of cubic phase stability in the simple MO/OG/water system (Fig. 5, *A* and *B*). And, it does so at the expense of the L_{α} phase. Presumably, then, this same transformation happens when salt is added to the in meso crystallization mix. Indeed, this has been confirmed by monitoring continuously the phase behavior of the bR-loaded in meso system through the crystallization process using x-ray diffraction (Fig. 6). Before salt is added and at a high bR loading, the phases present are of the L_{α} and cubic-Pn3m or cubic-Ia3d types (Fig. 6, *A* and *B*). With time after the addition of salt, the L_{α} phase disappears and the bulk

TABLE 1 Octyl glucoside depletion of solubilized bacteriorhodopsin and a control solution by treatment with Bio-Beads SM 2, determined by the diffraction-based detergent assay

| Incubation time with Bio-Beads (h) | Cubic-Pn3m lattice parameter (d_{100} , Å) | Estimated OG concentration* (M) |
|------------------------------------|---|---------------------------------|
| bR Solution | | |
| 0 | 108 | 0.51 |
| 0.5 | 105 | 0.42 |
| 1 | 94 | 0.09 |
| 2 | 94 | 0.09 |
| 3 | 93 | 0.06 |
| 4 | 92 | 0.03 |
| 5 | 92 | 0.03 |
| Control | | |
| 0 | 109 | 0.54 |
| 0.5 | 106 | 0.45 |
| 1 | 100 | 0.27 |
| 2 | 94 | 0.09 |
| 3 | 92 | 0.03 |
| 4 | 91 | 0.00 |
| 5 | 91 | 0.00 |

The control solution contained 0.46 M octyl glucoside in 25 mM Na/K phosphate, pH 5.6 are included.

*Detergent quantitation was based on the lattice parameter (d_{100}) of the cubic-Pn3m phase of the monoolein/water system prepared at high salt concentration (see Methods and Fig. 5 B). The following equation was used to convert d_{100} to OG concentration (M): $M = (d_{100} - 91)/33.4$. The estimated error on M is ± 0.09 M OG solution.

mesophase remaining is exclusively cubic-Pn3m (Fig. 6, C and D). Eventually bR crystals form from within the bulk cubic-Pn3m phase (Fig. 6, E and F).

High salt concentration effects

Data presented above demonstrate that high detergent concentrations destabilize the cubic phase and favor L_{α} phase formation. In the case of OG, this effect can be

reversed by raising salt concentration, as is typically done to effect protein crystal nucleation and growth in meso. The data in Fig. 7 show that the salt effect observed with OG is quite general. Thus, hydrated MO samples containing intermediate and high levels of all four alkyl glucosides used in this study, are initially in the L_{α} /cubic-Ia3d and L_{α} phases, respectively, and transform to the cubic-Pn3m phase when the salt concentration is raised.

DISCUSSION

Crystallizing membrane proteins by the in meso method typically involves an initial purification and solubilization in a mild, nonionic detergent such as OG. The protein dispersion/solution is combined with MO under conditions that spontaneously produce the cubic phase. In this way, the detergent becomes part of the crystallization mix. The purpose of this study was to quantify the effects of OG, and other commonly used detergents, on the phase behavior of hydrated MO with a view to evaluating its contribution to the crystallization process. Accordingly, the phase behavior and phase microstructure of the MO/detergent/water systems were characterized by small-angle x-ray diffraction.

The results presented in Figs. 1 and 2 show that the MO cubic phase has a limited capacity for added detergent. At low levels, the original cubic-Pn3m phase was retained and its capacity for added detergent rose with temperature, especially above 30°C. As detergent concentration increased, the cubic-Pn3m phase gave way to the cubic-Ia3d phase, which in turn transformed to the lamellar phase at higher levels of detergent. Undercooling of the liquid crystalline phases was observed down to 0°C.

Comparison with dodecyl maltoside and literature data

The results obtained with the alkyl glucosides used in this

TABLE 2 X-ray diffraction data for phase identification and microstructure characterization of the MO/OG/water system at 20°C prepared with either excess ammonium sulfate or excess Na/K phosphate, pH 5.6, and ammonium sulfate

| Na/K phosphate (M) | Ammonium sulfate (M) | OG solution concentration (M) | Relative amount of OG (mol/mol MO) | Cubic-Pn3m lattice parameter (d_{100} , Å) | Estimated OG concentration* (M) |
|--------------------|----------------------|-------------------------------|------------------------------------|---|---------------------------------|
| 0.0 | 1.8 | 0.42 | 0.10 | 101 | N/A [†] |
| 0.0 | 2.0 | 0.42 | 0.10 | 99 | N/A |
| 0.0 | 2.2 | 0.42 | 0.10 | 99 | N/A |
| 0.0 | 2.4 | 0.42 | 0.10 | 97 | N/A |
| 2.0 | 0.00 | 0.42 | 0.10 | 108 | 0.51 |
| 2.0 | 0.01 | 0.42 | 0.10 | 110 | 0.57 |
| 2.0 | 0.05 | 0.42 | 0.10 | 110 | 0.57 |
| 2.0 | 0.10 | 0.42 | 0.10 | 108 | 0.51 |
| 2.0 | 0.50 | 0.42 | 0.10 | 108 | 0.51 |

*Detergent quantitation was based on the lattice parameter (d_{100}) of the cubic-Pn3m phase of the monoolein/water system prepared at high salt concentration (see Methods and Fig. 5 B). The following equation was used to convert d_{100} to OG concentration (M): $M = (d_{100} - 91)/33.4$. The estimated error on M is ± 0.09 M OG solution.

[†]N/A; an estimation of OG concentration is not applicable in the absence of an excess of Na/K phosphate solution.

TABLE 3 X-ray diffraction data for phase identification and microstructure characterization of the MO/OG/water system at 20°C prepared with DOPE or DOPC

| Relative amount of additive (mmol/mol MO) | OG solution concentration (M) | Relative amount of OG (mol/mol MO) | Cubic-Pn3m lattice parameter (d_{100} , Å) | Estimated OG concentration* (M) |
|---|-------------------------------|------------------------------------|---|---------------------------------|
| DOPE | | | | |
| 7 | 0.21 | 0.05 | 99 | 0.25 |
| 7 | 0.42 | 0.10 | 106 | 0.46 |
| 20 | 0.21 | 0.05 | 102 | 0.33 |
| 20 | 0.42 | 0.10 | 112 | 0.62 |
| DOPC | | | | |
| 7 | 0.21 | 0.05 | 99 | 0.23 |
| 7 | 0.42 | 0.10 | 106 | 0.46 |
| 20 | 0.21 | 0.05 | 102 | 0.32 |
| 20 | 0.42 | 0.10 | 114 | 0.68 |

The phospholipid (DOPE or DOPC) was combined with the monoolein before cubic phase preparation.

*Detergent quantitation was based on the lattice parameter (d_{100}) of the cubic-Pn3m phase of the monoolein/water system prepared at high salt concentration (see Methods and Fig. 5 B). The following equation was used to convert d_{100} to OG concentration (M): $M = (d_{100} - 91)/33.4$. The estimated error on M is ± 0.09 M OG solution.

study are similar to those for DDM (Ai and Caffrey, 2000). This is not unexpected given that the detergents are all homologs. The corresponding phase diagrams for these systems are combined in Fig. 2 to facilitate comparison. A perusal of the data shows that the same phases occur in the same sequence as a function of temperature and detergent concentration. All of the boundaries slope in the same direction with increasing detergent concentration. There are some small differences in boundary positions with respect to temperature and composition. However, given that boundaries were hand-drawn to data collected at intervals of 5°C

TABLE 4 X-ray diffraction data for phase identification and microstructure characterization of the MO/OG/water system at 20°C prepared with lysozyme

| Lysozyme concentration (mg/ml) | OG solution concentration (M) | Relative amount of OG (mol/mol MO) | Cubic-Pn3m lattice parameter (d_{100} , Å) | Estimated OG concentration* (M) |
|--------------------------------|-------------------------------|------------------------------------|---|---------------------------------|
| 0 | 0.21 | 0.05 | 99 | 0.24 |
| 5 | 0.21 | 0.05 | 98 | 0.21 |
| 10 | 0.21 | 0.05 | 99 | 0.24 |
| 30 | 0.21 | 0.05 | 99 | 0.24 |
| 60 | 0.21 | 0.05 | 100 | 0.27 |

The protein was combined with the detergent solution before cubic phase preparation.

*Detergent quantitation was based on the lattice parameter (d_{100}) of the cubic-Pn3m phase of the monoolein/water system prepared at high salt concentration (see Methods and Fig. 5 B). The following equation was used to convert d_{100} to OG concentration (M): $M = (d_{100} - 91)/33.4$. The estimated error on M is ± 0.09 M OG solution.

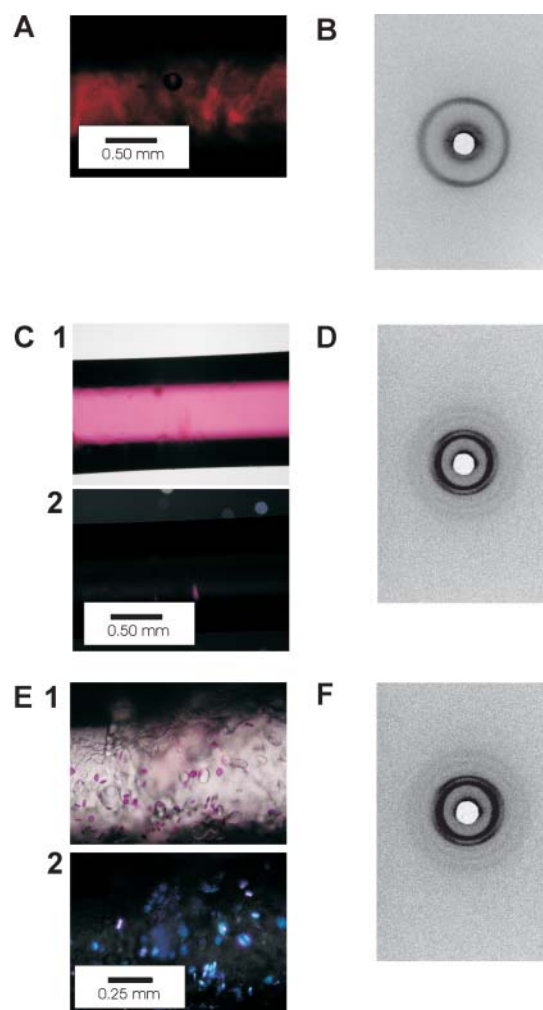


FIGURE 6 Mesophase behavior of the in meso system during the course of bacteriorhodopsin crystallization at 20°C. Shown in A, C, and E are x-ray capillaries containing the in meso mix viewed with a light microscope. The corresponding low-angle x-ray diffraction patterns recorded at 20°C are shown in B, D, and F, respectively. The data in A and B show that the crystallization mix shortly after preparation and before the addition of salt is a mixture of the L_{α} and cubic-Ia3d phases. After a 15-day equilibration with an excess of 2.5 M Na/K phosphate, pH 5.6, to initiate crystallization, the sample has transformed completely to the cubic-Pn3m phase (C and D). Bacteriorhodopsin crystals form with continued incubation and equilibration, and coexist with a bulk cubic-Pn3m (E and F, data recorded 15 days after the addition of salt). Images in panel 1 of C and in E were recorded with polarized light. Images in panel 2 of C and in E were recorded between crossed polarizers. Birefringence, characteristic of nonisotropic phases, is apparent in A. In C2 and E2, the bulk phase is isotropic (cubic) and appears dark and featureless between crossed polarizers. The birefringence in E2 is from the bR crystals. Samples were prepared with 60% (w/w) monoolein and 40% (w/w) bR solution at 21.2 mg protein/mL in all cases.

and ≥ 0.03 M, the errors in boundary location are of a magnitude to suggest that the differences seen are not significant.

The comparison in Fig. 2 is made on the basis of molar detergent concentrations. It is important to note that the molecular weights of the detergents differ. For example, the

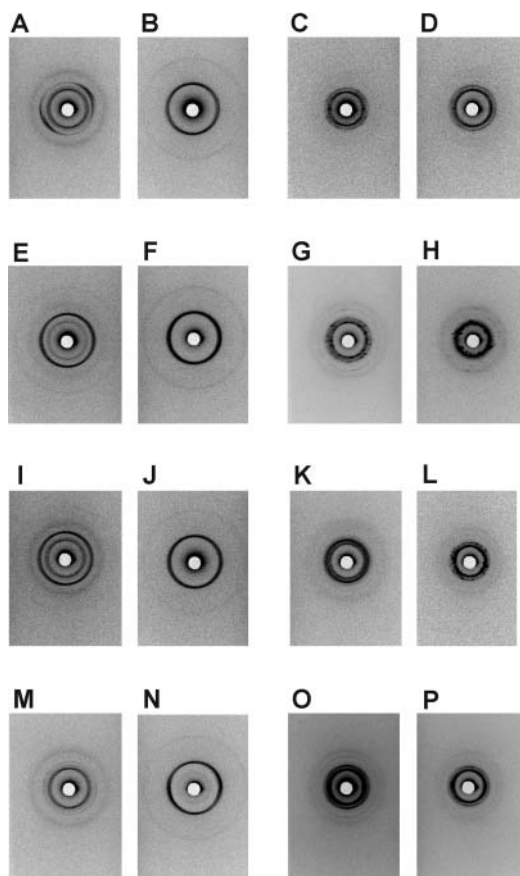


FIGURE 7 Detergents trigger a cubic-to-lamellar phase transition in hydrated monoolein that is reversed at high salt concentration. Low-angle diffraction patterns were recorded at 20°C at low (0.3 M detergent solution) and high (0.5 M detergent solution) concentrations of detergent, respectively, for hexyl glucoside (*A* and *B*), octyl glucoside (*E* and *F*), nonyl glucoside (*I* and *J*), and decyl glucoside (*M* and *N*), in the absence of salt. After equilibration with 2.0 M Na/K phosphate, pH 5.6, all of the samples converted to the cubic-Pn3m phase at low and high concentrations of hexyl glucoside (*C* and *D*), octyl glucoside (*G* and *H*), nonyl glucoside (*K* and *L*), and decyl glucoside (*O* and *P*), respectively. Samples, prepared with 60% (w/w) monoolein and 40% (w/w) detergent solution in x-ray capillaries, were used directly for diffraction measurements in the absence of salt. Subsequently, the lipid dispersions were overlaid with 2.0 M Na/K phosphate, pH 5.6, and the samples were incubated for seven days at room temperature before phase determination measurements by x-ray diffraction.

molecular weight of DDM (511 g/mol) is almost twice that of OG (292 g/mol). Thus, in the simplest case where densities are all unity and volumes are additive, the water content in % (w/w) of an OG solution is greater than that of an equimolar DDM solution. Accordingly, a 0.5 M OG solution has 85% (w/w) water compared to 74% (w/w) water in the case of an equimolar DDM solution. These translate, respectively, to 34 and 30% (w/w) actual water content in the samples used in this study that were prepared with three parts (by weight) lipid and two parts detergent solution. The disparity lessens at lower detergent concentrations. Since the overall detergent concentrations under consideration are

relatively low, and in light of boundary location uncertainty, the net effect on water content is not sufficiently large to impact significantly on relative boundary positions. Nonetheless, it is worth noting that the mesophase behavior of such systems is profoundly sensitive to level of hydration (the so-called lyotropic effect) as illustrated in the temperature-composition phase diagram of the MO/water system (Qiu and Caffrey, 2000).

The phase behavior of the hydrated MO/OG system has been investigated recently (Persson et al., 2003). A comparison with the current work is difficult because very different protocols were employed. In the Persson et al. study, rapid heating and cooling rates of 60 and 300°C/h, respectively, were employed. In the current work, each sample was incubated for at least 3 h at a given temperature before making a measurement (see Methods). Further, in the Persson et al. study unusual behaviors such as strong and sharp, but unidentified, reflections as well as unusual line broadening and phase coexistence were observed with some frequency in the diffraction measurements. For these reasons, plus the fact that mesophase transitions and unit cell size equilibrations can be tardy (Caffrey, 1989), quantitative comparisons of the Persson et al. study and the current study are not warranted. Nonetheless, a perusal of the data shows qualitative agreement.

In a study by Sennoga et al. (2003), a series of alkyl glycosides and a thioglycoside were examined for compatibility with a model system for use in in meso crystallization. The work is similar to that of Persson et al. (2003), already discussed, and to extensive earlier work from this lab on DDM (Ai and Caffrey, 2000). In the Sennoga et al. study sample incubation protocols more closely followed those used in our work with a minimum sample preincubation time of 2 h. Thus, where comparisons can be made, the two studies are in reasonable agreement. In Sennoga et al. (2003), considerable emphasis is placed on the prospect of using an undercooled cubic phase for in meso crystallization at low temperature. We caution, however, that the undercooled condition is intrinsically unstable and can transform at any time to an equilibrium state that may not be compatible with crystal growth (Caffrey, 2003). One additional point worth noting in regard to the Sennoga et al. (2003) findings is that they refer to a simple model system. As shown in the current work, the addition of salt, as is typically done under crystallization screen conditions, should serve to enhance the stability of the cubic phase.

Relevance to crystallization

Since the mechanism of membrane protein crystallization in meso is not known, it is inappropriate to make recommendations as to limits on detergent concentrations for use in the crystallization mix. The cubic phase figures prominently in the method but the particular cubic phase type (as in space group Pn3m or Ia3d, etc.) preferred has not been identified

(Caffrey, 2003). When such a determination has been made, it will be possible to consult the phase diagrams in Fig. 2 and to choose an appropriate alkyl glycoside concentration for use at a given temperature. Further, to recommend avoiding the lamellar phase completely, and thus high alkyl glycoside concentrations, may not be appropriate either because, as noted, it may play a role as a protein portal between the crystal and the bulk cubic phase. Accordingly, small amounts of detergent that facilitate local lamellar phase formation may in fact favor the crystallization process. When in meso crystallization is performed in the absence of added detergent, MO has been proposed to act as a surrogate (Caffrey, 2000).

The entire suite of liquid crystal phases observed in this study in the presence of alkyl glycosides exists in the undercooled state down to 0°C. This has implications for performing in meso crystallization at temperatures below that (room temperature, 20°C) at which the original method was developed. It is important to realize, however, that if crystallization trials are performed in the 0–18°C range, the system is intrinsically unstable and that it can revert at any time to the stable, equilibrium solid (Lc) phase. Lc phase formation is likely to disrupt the crystallization process. We are currently in search of other lipids that behave like MO with regard to in meso crystallization but that have a true equilibrium cubic phase in the 0–20°C range (Misquitta and Caffrey, 2001).

In this study, we have shown that high salt concentration can be used to “recover” the cubic phase that transforms partially or completely to the L_{α} phase in the presence of detergent. Thus far, there is no evidence to show that membrane proteins grow from anything other than a bulk cubic phase. This statement does not exclude the possibility that a local lamellar portal exists between the bulk cubic phase and the face of the crystal, as noted. Nor indeed is there any evidence that crystals grow from any other bulk mesophase. Our working model therefore is that the cubic phase is integral to the crystallization process. Crystallization trials involve sampling myriad environmental and compositional conditions. With regard to the latter, many crystallization screen additives have the capacity to destabilize the cubic phase. A survey of commonly used commercial screens for their effects on cubic phase stability has been reported (Cherezov et al., 2001). An important point that emerges from the current work is that although a particular additive may destabilize the cubic phase, it does not necessarily mean that the system is useless in in meso crystallization trials. What presumably is critical to the success of the method is that the cubic phase be restored for crystal nucleation and growth. Thus, the added salt may serve double duty under such situations. On the one hand, it reverses the transition from the cubic to the lamellar phase induced by the additive, detergent, for example. On the other, it facilitates crystal nucleation and growth by raising bilayer curvature and by charge screening, as described

(Caffrey, 2000). These results serve to emphasize the need to evaluate compositional and environmental effects on the in meso system under conditions as close as possible to those prevailing during crystallization, as has been done in this study.

Further, whereas the protein may be stable for an extended period in the cubic phase, there is no guarantee that stability will prevail in the lamellar (L_{α}) phase. Success with crystallizing the native state of a membrane protein is likely therefore to benefit from knowing mesophase behavior and propensity under the range of conditions to be explored in a given crystallization trial. This study contributes to that knowledge base.

In the old literature dealing with fats and liquid crystals, the cubic phase was referred to as the “viscous isotropic” phase. The isotropic feature refers to its interaction with light and its nonbirefringent properties. Extreme viscosity is one of its other characteristics. This presents practical challenges at two stages in in meso crystallization. The first has to do with the preparation and manipulation of the phase which, of course, does not lend itself to conventional liquid handling. An inexpensive mechanical mixing and delivery device has been developed for this purpose (Cheng et al., 1998). The second problem arises in recovering crystals from within the viscous cubic phase for mounting and diffraction data collection. One solution exploits certain mesophase properties highlighted in this and earlier related work. It transpires that the L_{α} phase is considerably less viscous than its cubic counterpart. Thus, as emphasized in the current study, judiciously flooding the system with detergent should lead to a cubic-to-lamellar phase transition and to more readily retrievable crystals. This principle has been implemented and shown to work in practice (Luecke et al., 1999).

Detergent assay

In the course of this work, an earlier observation that the unit cell size of the cubic phase rises with DDM concentration was shown to be quite general. The effect was observed with three other alkyl glucosides (unpublished work) and with LDAO under conditions where an excess of aqueous medium is available. To a first approximation, the dependence of cubic phase lattice parameter on detergent concentration is linear. At high salt concentration, the linear range extends to 0.93 M detergent concentration in the case of OG and a little higher in the case of LDAO. The assay works well under a host of compositional conditions typically encountered with detergent-containing samples. These include moderate concentrations of the salt ammonium sulfate, the water-soluble protein lysozyme, and the glycerophospholipids, DOPC and DOPE.

Other detergent assay methods exist. They include the use of radiolabeled detergents (Le Maire et al., 1983), Fourier transform infrared spectroscopy (daCosta et al., 2003), and

TLC (Eriks and Kaplan, 2003). For sugar-containing detergents, a modification of the original phenol-sulfuric acid method for sugar determination (Dubois et al., 1956) has been implemented (Lau and Bowie, 1997). Each of these methods has its advantages and disadvantages. The value to us of the diffraction-based method is that it is convenient since we perform such measurements routinely.

CONCLUSIONS

The partial temperature-composition phase diagrams of four MO/alkyl glucoside/water systems have been constructed using x-ray diffraction in the cooling direction. In the case of the OG system, data were collected under both heating and cooling conditions. The solid Lc phase dominates the heating phase diagram below 20°C over the full range of OG solution concentrations (0–0.6 M) examined. At and above 20°C, liquid crystal phases emerge whose identity and phase microstructure are temperature- and detergent concentration-dependent. Under conditions of undercooling, the liquid crystal phases persist to 0°C for all alkyl glucosides examined in this study.

With these phase diagrams in place, it is now possible to make definitive statements as to how the alkyl glucoside detergents affect phase behavior, and how the effects change with temperature. The microstructure data show that detergent and temperature can be used to fine-tune the lattice dimensions of the different phases accessed. This latter feature will become significant in a practical sense as the range of membrane proteins subjected to in meso crystallization grows.

The hydrated MO cubic phase was shown to be relatively robust with regard to phase stability and alkyl glucoside addition. Thus, small amounts of the detergents were tolerated by the cubic phase. Higher levels, however, induced a transformation to the lamellar phase. This effect makes good sense when viewed from the perspective of the interacting lipid and detergent contributing complementary molecular shapes that stabilize a planar lamellar phase (Ai and Caffrey, 2000).

The carrying capacity of the hydrated MO cubic phase for alkyl glucosides and LDAO rises substantially at high salt concentrations. This finding has implications for membrane protein crystallization in meso, which is usually performed at high salt concentrations.

The unit cell size of the cubic phase in hydrated MO is sensitive to detergent concentration. This sensitivity, which is linear up to ~1.0 M in the case of OG and LDAO, forms the basis of a detergent assay. The assay is relatively insensitive to salt (ammonium sulfate), lipid (DOPC, DOPE), and protein (lysozyme).

SUPPLEMENTARY MATERIAL

An online supplement to this article can be found by visiting BJ online at <http://www.biophysj.org>.

We thank V. Cherezov for invaluable input to this study and W. Abd el-Gawad for contributions to parts of this work.

This study was funded by the National Institutes of Health (GM61070) and the National Science Foundation (DIR9016683 and DBI9981990).

REFERENCES

- Ai, X., and M. Caffrey. 2000. Membrane protein crystallization in lipidic mesophases: detergent effects. *Biophys. J.* 79:394–405.
- Briggs, J., H. Chung, and M. Caffrey. 1996. The temperature-composition phase diagram and mesophase structure characterization of the monoolein/water system. *J. Phys. II France.* 6:723–751.
- Caffrey, M. 1987. Kinetics and mechanism of transitions involving the lamellar, cubic, inverted hexagonal, and fluid isotropic phase of hydrated monoacylglycerides monitored by time-resolved x-ray diffraction. *Biochemistry.* 26:6349–6363.
- Caffrey, M. 1989. The study of lipid phase transition kinetics by time-resolved x-ray diffraction. *Annu. Rev. Biophys. Biophys. Chem.* 18:159–186.
- Caffrey, M. 2000. A lipid's eye view of membrane protein crystallization in mesophases. *Curr. Opin. Struct. Biol.* 10:486–497.
- Caffrey, M. 2002. Membrane form and function in finer focus. *Curr. Opin. Struct. Biol.* 12:471–479.
- Caffrey, M. 2003. Membrane protein crystallization. *J. Struct. Biol.* 142:108–132.
- Cheng, A., B. Hummel, H. Qiu, and M. Caffrey. 1998. A simple mechanical mixer for small viscous samples. *Chem. Phys. Lipids.* 95:11–21.
- Cherezov, V., and M. Caffrey. 2003. Nano-volume plates with excellent optical properties for fast, inexpensive crystallization screening of membrane proteins. *J. Appl. Cryst.* In press.
- Cherezov, V., H. Fersi, and M. Caffrey. 2001. Crystallization screens: compatibility with the lipidic cubic phase for in meso crystallization of membrane proteins. *Biophys. J.* 81:225–242.
- Cherezov, V., J. Clogston, Y. Misquitta, W. Abdel-Gawad, and M. Caffrey. 2002. Membrane protein crystallization in meso: lipid type-tailoring of the cubic phase. *Biophys. J.* 83:3393–3407.
- daCosta, C. J. B., and J. E. Baenziger. 2003. A rapid method for assessing lipid: protein and detergent: protein ratios in membrane-protein crystallization. *Acta Cryst. D.* 59:77–83.
- Dencher, N. A., and M. P. Heyn. 1982. Preparation and properties of monomeric bacteriorhodopsin. *Methods Enzymol.* 88:5–10.
- Dubois, M., K. A. Gilles, J. K. Hamilton, P. A. Rebers, and F. Smith. 1956. Colorimetric method of determination of sugars and related substances. *Anal. Chem.* 28:350–356.
- Eriks, L. R., and R. S. Kaplan. 2003. The development of a novel strategy for identification and quantification of detergents commonly used for the purification of membrane proteins. *Biophys. J.* 84:352a.
- Hunte, C., and H. Michel. 2003. Membrane protein crystallization. *In* Membrane Protein Purification and Crystallization. A Practical Guide. C. Hunte, G. von Jagow, and H. Schagger, editors. Academic Press, New York. 143–160.
- Lau, F. W., and J. U. Bowie. 1997. A method for assessing the stability of a membrane protein. *Biochemistry.* 36:5884–5892.
- Le Maire, M., S. Kwee, J. P. Andersen, and J. V. Moeller. 1983. Mode of interaction of polyoxyethyleneglycol detergents with membrane proteins. *Eur. J. Biochem.* 129:525–532.
- Luecke, H., B. Schobert, H.-T. Richter, J.-P. Cartailleur, and J. K. Lanyi. 1999. Structure of bacteriorhodopsin at 1.55 Å resolution. *J. Mol. Biol.* 291:899–911.
- Misquitta, Y., and M. Caffrey. 2001. Rational design of lipid molecular structure: a case study involving the C19:1c10 monoacylglycerol. *Biophys. J.* 81:1047–1058.

- Nollert, P., H. Qiu, M. Caffrey, J. P. Rosenbusch, and E. M. Landau. 2001. Molecular mechanism for the crystallization of bacteriorhodopsin in lipidic cubic phases. *FEBS Lett.* 504:179–186.
- Persson, G., H. Edlund, and G. Lindblom. 2003. Thermal behaviour of cubic phases rich in 1-monooleoyl-*rac*-glycerol in the ternary system 1-monooleoyl-*rac*-glycerol/n-octyl- β -D-glucoside/water. *Eur. J. Biochem.* 270:56–65.
- Qiu, H., and M. Caffrey. 2000. The phase diagram of the monoolein/water system. Equilibrium and metastability aspects. *Biomaterials.* 21:223–234.
- Rummel, G., A. Hardmeyer, C. Widmer, M. L. Chiu, P. Nollert, K. P. Locher, I. Pedruzzi, E. M. Landau, and J. P. Rosenbusch. 1998. Lipidic cubic phases: new matrices for the three-dimensional crystallization of membrane proteins. *J. Struct. Biol.* 121:82–91.
- Sennoga, C., A. Heron, J. M. Seddon, R. H. Templer, and B. Hankamer. 2003. Membrane-protein crystallization in cubo: temperature-dependent phase behaviour of monoolein-detergent mixtures. *Acta Crystallogr. D.* 59:239–246.